Geophysical Prospecting, 2007, **55**, 265–275

Estimation of clay content in soil based on resistivity modelling and laboratory measurements

Vladimir Shevnin*, Aleksandr Mousatov, Albert Ryjov and Omar Delgado-Rodriquez

Mexican Petroleum Institute, Eje Central Lazaro Cardenas 152, Col. San Bartolo Atepehuacan 07730, Mexico

Received April 2004, revision accepted August 2006

ABSTRACT

The determination of clay content in near-surface formations is crucial for geotechnical, hydrogeological and oil-contamination studies. We have developed a technique for estimating clay content that consists of the minimization of the difference between the theoretically calculated and measured soil resistivities as a function of water salinity. To calculate the resistivity, we used a model that takes into account the electrochemical processes in the clay micropores. The experimental measurements of soil resistivity were performed on soil samples, completely saturated by brines at different concentrations of NaCl salt in the range 0.6–100 g/l, to obtain the resistivity versus salinity curve. The parameters obtained with this curve inversion are the clay content, the total porosity and the cation exchange capacity. To verify the new technique, we determined clay concentrations of artificial mixtures of calibrated sand and clay. The relative mean error in the clay content does not exceed 20% for a 5% fitting error of the resistivity versus salinity curves. Such evaluations allow the correct separation of the main lithological groups (sand, sandy loam, loam, and light, medium and heavy clay).

We applied this technique to estimate the petrophysical parameters of soils (clay content, porosity and cation exchange capacity) at various sites in Mexico. The results improved the interpretation of the vertical electrical soundings, the lithological soil characterization and the delineation of oil-contaminated areas.

INTRODUCTION

Soil resistivity depends on petrophysical parameters, such as pore microstructure, pore volume, pore-fluid saturation and fluid type. Generally, the shallow part of the subsurface consists of weakly consolidated soils composed of sand and clay mixtures. Clay-content determination is required for an adequate site characterization and to solve geotechnical, hydrogeological and ecological problems. Vertical electrical sounding and electrical imaging are widely applied for the study of near-surface structures and soil properties down to depths of 20–30 m. The resistivity method is sensitive to the presence of clay due to electrochemical processes. This implies that, potentially, we could obtain the clay parameters (clay content and cation exchange capacity) from resistivity data.

A resistivity model that considers the influence of clay on the bulk conductivity of porous rocks was proposed by Waxman and Smits (1968), based on experimental data obtained in the petroleum industry for water and oil-bearing shaly sands. They found that the bulk conductivity depends on the sum of the pore-water conductivity and a surface conductivity related to the cation exchange capacity of clay minerals. This model was modified by Clavier, Coates and Dumanoir (1984), who introduced a dual-water model in which the rock conductivity was presented as a function of the bulk pore electrolyte and clay water in the electrical double layer on the clay particles. An empirical law for the conductivity of shaly sand formations with different surface and bulk tortuosities was introduced by Sen and Goode (1988). The theoretical studies performed by

*E-mail: vshevnin@imp.mx

Johnson and Sen (1988) and Tabbagh *et al*. (2002) demonstrated that the effective conductivity of a porous medium can be expressed as the sum of two conductivities related to the surface and bulk conduction mechanisms.

Using the Bruggeman–Hanai equation, Bussian (1983) proposed a model that explains the behaviour of sedimentary-rock conductivity, using the geometry of a two-component system composed of the pore-water host and conductive solid inclusions. This approach was further extended by de Lima and Sharma (1990) and Samstag and Morgan (1991). A theoretical study of surface conductivity was performed by Revil and Glover (1998). Using the differential effective-medium theory and the Bussian approach, Revil *et al*. (1998) developed an electrical-conductivity equation that includes the ionic composition of the pore water and the electrical double layer.

Rhoades *et al*. (1976), Ryjov (1987) and Ryjov and Sudoplatov (1990) proposed a conductivity model for sand-clay mixtures, taking into account both the geometrical microstructure and electrochemical process for wide ranges of water salinity and clay concentrations.

The technology of measuring electrical properties on consolidated (hard) rocks is well-developed and was used to study completely and partially water-saturated samples (Knight 1991; Taylor and Barker 2002). Klein and Santamarina (1997, 2003) studied different methods of electromagnetic measurements in a broad frequency range for soil-water mixtures, and demonstrated that surface conductivity significantly affects the bulk electrical conductivity in soils saturated with pore fluids of low ionic concentration.

We present a technique for determining the properties of weakly consolidated clay soils that consist of a mixture of sand and clay. Structural clay is seldom found in soils and is therefore ignored in this study. The estimation of clay concentration, cation exchange capacity and porosity includes inversion of the electrical resistivity curve of soil, which was measured for several values of water salinity.

RESISTIVITY MODEL OF A SANDY-CLAY SOIL MIXTURE

The original method for the soil-resistivity calculation used in this work was proposed by Ryjov (1987) and Ryjov and Sudoplatov (1990). The soil microstructure model is treated as a porous heterogeneous medium composed of sand grains and clay particles (Fig. 1). The sand component contains a porous system of cylindrical channels (so-called wide pores) with radii of 10^{-3}-10^{-4} m, which are much larger than the thickness

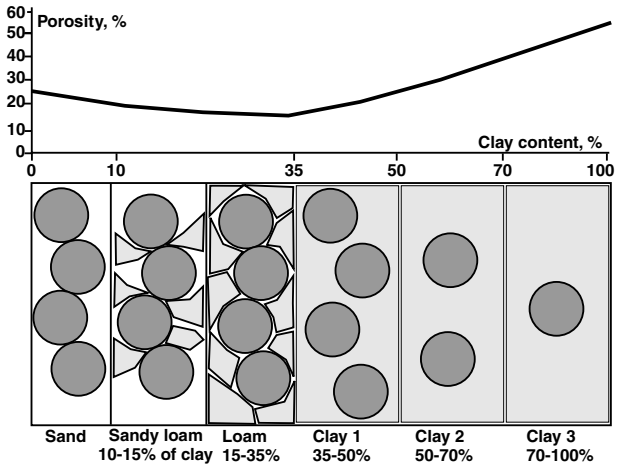

Figure 1 Model of soil for different clay contents.

of the electrical double layer. The thickness of the electrical double layer depends on the water salinity and increases with decreasing salt concentration. At near-surface conditions, when the salt concentration changes from 0.02 to 2 g/l, the thickness of the electrical double layer varies in the range of $0.3–3 \times 10^{-8}$ m. The micropores of the clay component are very narrow, and their average radii lie between 10^{-7} and 10^{-8} m, which is close to the thickness of the electrical double layer. In this model, the walls of both wide and fine capillaries are considered non-conductive, and are characterized by electrochemical parameters, such as the electrical double layer and the cation exchange capacity. The pores can be partially or completely saturated by brine. Thus, in this approach, electrical properties of the sand-clay mixture are defined by the effective conductivities of both wide and fine capillary systems, and by the interconnections of these two pore networks.

The conductivities of the sand (σ_{sand}) and clay (σ_{clay}) components can be written as follows:

$$\sigma_{\text{sand}} = \phi_{\text{sand}}\sigma_{\text{sandcap}}, \tag{1}$$

$$\sigma_{\text{clay}} = \phi_{\text{clay}}\sigma_{\text{claycap}}, \tag{2}$$

where σ_{sandcap} and σ_{claycap} are the conductivities of single sand or clay capillaries, respectively, and ϕ_{sand} and ϕ_{clay} are the porosities of the sand and clay components, expressed as volume fractions of the total volume.

The average conductivity $\tilde{\sigma}_{\text{cap}}$ of a capillary completely saturated by brine can be considered as a radially varying function $\sigma\,(r)$ that depends on the electrical double layer properties

(thickness and counterion concentration):

$$\tilde{\sigma}_{\text{cap}} = \frac{2}{r_c^2} \int_0^{r_c} r\sigma(r)\,\mathrm{d}r, \tag{3}$$

where r_c is the capillary radius.

In partially saturated soils, the non-conductive phase (air, oil, gas or ice) occupies the central part of the pores because soils are generally water-wet. In this case, the equation becomes

$$\tilde{\sigma}_c = \frac{2}{r_c^2} \int_{r_w}^{r_c} r\sigma(r)\,\mathrm{d}r, \tag{4}$$

where $r_w = r_c\sqrt{1 - S_w}$ is the internal radius of the water film in capillaries and S_w is the water saturation expressed as a fraction of the total pore volume.

In the pore system of the sand, which has wide capillaries, the average conductivity of sand channels σ_{sandcap} does not depend on capillary radius and corresponds to the free-water conductivity σ_w. The conductivity of water solutions, without and with the influence of capillary walls, depends on salt concentration, anion and cation properties, and the influence of the electric double layer (see Appendix).

THE INFLUENCE OF SOIL STRUCTURE PARAMETERS

The microstructure of clay-rich shallow soils can be described using an ideal packing concept for binary mixtures of fine and coarse particles of quasi-spherical shapes (McGeary 1961). According to this model, while the clay fraction is less than the sand porosity, the clay particles (which have an average radius much smaller than that of the sand grains) will fit within the sand pores and will not change the sand structure. When the clay fraction exceeds the sand porosity, the sand grains become suspended in the clay host.

The total porosity ϕ_t of the sandy-clay soil reflects the properties of a binary mixture (Fig. 1) and can be approximated by the following expressions (Ryjov and Sudoplatov 1990; Marion *et al*. 1992; Revil, Grauls and Brévart 2002):

$$\phi_t = (\phi_{\text{sand}} - C_{\text{clay}}) + \phi_{\text{clay}} C_{\text{clay}}, \quad \text{when } C_{\text{clay}} < \phi_{\text{sand}}, \tag{5}$$

$$\phi_t = C_{\text{clay}}\phi_{\text{clay}}, \quad \text{when } C_{\text{clay}} \geq \phi_{\text{sand}}, \tag{6}$$

where C_{clay} is the volumetric clay content (fraction) in a sand-clay mixture.

When $C_{\text{clay}} > \phi_{\text{sand}}$, the total conductivity of soil, σ_Σ, corresponds to the effective conductivity of the clay component and depends on the conductivity of narrow channels (σ_{claycap}), clay porosity and salt concentration. The sand component will, in this case, only diminish the volume of the clay host (C_{clay}):

$$\sigma_\Sigma = \sigma_{\text{claycap}} C_{\text{clay}} \phi_{\text{clay}}, \quad \text{when } C_{\text{clay}} > \phi_{\text{sand}}. \tag{7}$$

When $C_{\text{clay}} < \phi_{\text{sand}}$, the soil conductivity is defined by both the sand pore system and fine clay capillaries saturated by water of a given salinity. The interconnections of pore networks can be considered as circuits connected in parallel or series. The soil element with parallel capillaries has conductivity given by

$$\sigma_{\text{prl}} = \sigma_{\text{claycap}}\phi_{\text{clay}} C_{\text{clay}} + \sigma_{\text{sandcap}}(\phi_{\text{sand}} - C_{\text{clay}}), \tag{8}$$

where σ_{prl} is a conductivity of a soil element consisting of a sand-clay mixture and parallel connections of capillaries.

The soil element with series connection of sand and clay capillaries has conductivity given by

$$\sigma_{\text{ser}} = \left[\left(1 - \frac{C_{\text{clay}}}{\phi_{\text{sand}}}\right) \frac{1}{\phi_{\text{sand}}\sigma_{\text{sandcap}}} + \frac{C_{\text{clay}}}{\phi_{\text{sand}}} \frac{1}{\phi_{\text{sand}}\phi_{\text{clay}}\sigma_{\text{claycap}}} \right]^{-1}. \tag{9}$$

In nature, the combination of both parallel and series capillaries is generally observed, because some part of the clay is usually smeared on pore walls of the sand fraction, and some clay exists in the sand pores as plugs. The parallel and series connections of the conductive component were considered in the resistivity models developed by Wyllie and Southwick (1954) and Bussian (1983). To account for this, we split capillaries into a volumetric part of parallel capillaries equal to M and a serial part equal to $1 - M$. In this case, it is possible to calculate the total conductivity of soil with the following formula:

$$\sigma_\Sigma = M\sigma_{\text{prl}} + (1 - M)\sigma_{\text{ser}}, \quad \text{when } C_{\text{clay}} < \phi_{\text{sand}}, \tag{10}$$

where the conductivity σ_Σ includes the combination of parallel and series connections of capillaries.

Such an approach allows a variety of sand and clay combinations at low clay content ($C_{\text{clay}} < \phi_{\text{sand}}$). For example, we can consider a mixture with 10% of clay in the form of plugs, and the other 90% of the clay coating the walls ($M = 0.9$). A similar approach was used by Marion and Nur (1991) for describing the elastic properties of porous fluid-filled media. The analysis of the relationships between M and the clay microstructures of soil was published by Ryjov and Sudoplatov (1990).

To include the influence of the pore microstructure in the model, we have taken into account the tortuosity of the sand

pores as a function of the content of solid sand grains in the mixture. In resistivity models of rock, the pore tortuosity is generally accounted for through the formation factor, which is a non-linear function of porosity (Waxman and Smits 1968; Clavier *et al*. 1984; Sen and Goode 1988). In the widely accepted Archie's law, the effective conductivity σ^* of a porous isotropic medium is given by

$$\sigma^* = \phi^m \sigma_w, \tag{11}$$

where ϕ is the total medium porosity, m is the cementation exponent, and σ_w is the conductivity of water that completely fills the pore system in either sand or clay.

Introducing the pore tortuosity as the geometrical factor G, this formula can be rewritten as

$$\sigma^* = G\phi\sigma_w. \tag{12}$$

In geophysics, the tortuosity G is generally expressed as a function of the medium porosity,

$$G = \phi^k, \tag{13}$$

where $k = m - 1$.

When pores are saturated by the multicomponent material, the geometrical factor should be presented through the concentration of the solid non-conductive component. In the case of sand and clay mixtures, G has the same constant value,

$$G = \phi_{sand}^k, \tag{14}$$

if the clay concentration is less than the sand porosity ($C_{clay} = \phi_{sand}$), and it increases up to 1 when $C_{clay} > \phi_{sand}$ (Fig. 1), i.e.

$$G = C_{clay}^k. \tag{15}$$

We have assumed that the value of the exponent k is 1/2, based on the results presented by Sen, Scala and Cohen (1981). Using the differential effective-medium approach, they demonstrated that the cementation exponent m of unconsolidated glass beads is 1.5.

Taking into account the fact that, in our model, the mixture conductivity σ_Σ, given by equations 7,8,9,10, corresponds to the product $\phi\sigma$ in expression (12), i.e. $\sigma^* = G\sigma_\Sigma$, we have obtained the final formulae for the calculation of the effective conductivity of sandy-clay soil, i.e.

$$\sigma* = \sqrt{\phi_{sand}}\sigma_\Sigma, \quad \text{when } C_{clay} \le \phi_{sand}, \tag{16a}$$

$$\sigma* = \sqrt{C_{clay}}\sigma_\Sigma, \quad \text{when } C_{clay} > \phi_{sand}. \tag{16b}$$

In the theory, we used the conductivity σ, but for practical applications it is more convenient to use the resistivity ρ, which is equal to $1/\sigma$. Numerical simulation of the resistivity

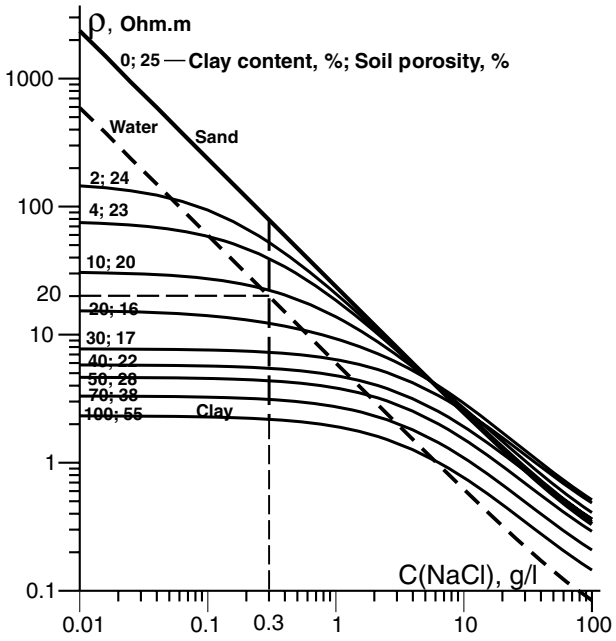

Figure 2 Theoretical dependence of the resistivity of a sandy-clay mixture on groundwater salinity. Clay porosity = 55%, sand porosity = 25%, $r_{sand} = 10^{-4}$ m, $r_{clay} = 10^{-8}$ m, $CEC_{clay} = 3$ g/l, $CEC_{sand} = 0$. Lithology legend for C(NaCl) = 0.3 g/l: sand: 30–80 Ωm, sandy loam: 13–30 Ωm, loam: 8–13 Ωm, light clay: 5–8 Ωm, medium clay: 3–5 Ωm, heavy clay: 2–3 Ωm.

of sandy-clay mixtures and the dependence on groundwater salinity is based on the formulae (7)–(10) and (16). An example of the results is shown in Fig. 2. (The values on curves indicate clay content in percentage from 0 (sand) up to 100 (clay) and soil porosity in percentage.) The inclined dashed line indicates the water resistivity. If we know, for example, that the groundwater resistivity is 20 Ωm, we can estimate the water salinity (0.3 g/L) from Fig. 2, and create a lithological table in which each type of soil (sand, sandy loam, loam and light, medium and heavy clay) has its own resistivity interval. Knowing the groundwater and soil resistivities, we can estimate, with the help of Fig. 2, the soil lithological composition, clay content and soil porosity. In practice, we use the inversion for estimating these parameters.

LABORATORY MEASUREMENTS OF SOIL RESISTIVITY

The laboratory measurements include the determination of soil resistivity as a function of pore-water salinity. For this purpose, we divided the soil sample into 3–5 subsamples, each of which was completely saturated with fluid of a different

salt concentration, from 0.6 to 100 g/L. We then measured the resistivity of each subsample using identically calibrated soil resistivimeters.

DATA INVERSION AND SENSITIVITY ANALYSIS

To determine the clay parameters of soils, we inverted the curves of soil resistivity as a function of water salinity obtained by laboratory measurements, minimizing the difference between the experimentally obtained resistivities ρ^{e} and theoretically calculated resistivities ρ^{t} defined by the standard rms fitting error.

The theoretical curve is calculated using equations 7,8,9,10 and 16. With the inversion, we estimated clay content, total porosity, cation exchange capacity (CEC) and clay capillary radius r_c. All these properties are arguments of the parameter vector p.

To estimate the influence of the soil parameters on the inversion results, we carried out a sensitivity analysis, which is well-known in inversion theory (Goltsman 1971; Tarantola 1994). For this purpose, the non-linear forward problem is linearized and converted into a system of linear algebraic equations. The inverse problem solution is found by calculating the corrections Δp to the parameter vector p corresponding to the system,

$$\mathbf{x} = \mathbf{\Phi}^{-1}\mathbf{y}, \tag{17}$$

where y is the vector of the relative differences between the theoretical ρ^{t} and experimental ρ^{e} curves with elements, $y_i = \frac{\rho_i^{e} - \rho_i^{t}}{\rho_i^{t}}$; $\times$ is the vector of the relative corrections in parameters with elements, $x_j = \frac{\Delta p_j}{p_j}$; p_j is any parameter of the model; Φ is the matrix of the logarithmic partial derivatives of the field ρ^{t} with elements, $\Phi_{ij} = \frac{\partial \ln \rho_i^{t}}{\partial \ln p_j}$; Φ^{-1} is the inverse Φ.

We applied the sensitivity analysis to the algorithm of soil-resistivity calculations, considering parameters such as sand and clay porosities, clay content, humidity, cation exchange capacity and clay capillary radii. The sensitivity as a function of the water salinity was calculated numerically for two models with clay contents of 10% and 50%, as shown in Fig. 3.

In the case of the 10% clay model, the list of parameters in descending order of influence on the sensitivity function is as follows: the humidity (19 r.u., here r.u. denotes relative dimensionless unit), sand porosity (9 r.u), clay porosity (8 r.u), clay capillary radii (3.8 r.u), clay content (2.7 r.u) and finally CEC (2.4 r.u). For the 50% clay model, the list of parameters is: clay porosity (18 r.u), humidity (16 r.u), clay content (11.2 r.u), clay capillary radii (5.5 r.u) and CEC (3.3 r.u). The sand porosity has no influence on the 50% clay model. If we exclude humidity from the list of parameters (by fixing it at 100%), we find that the sand and clay porosities for the 10% clay model and the clay porosity and clay content for the 50% clay model are the parameters with the largest influence.

The influence of temperature on resistivity is equal for all salinities. This allows us to transform the theoretical and

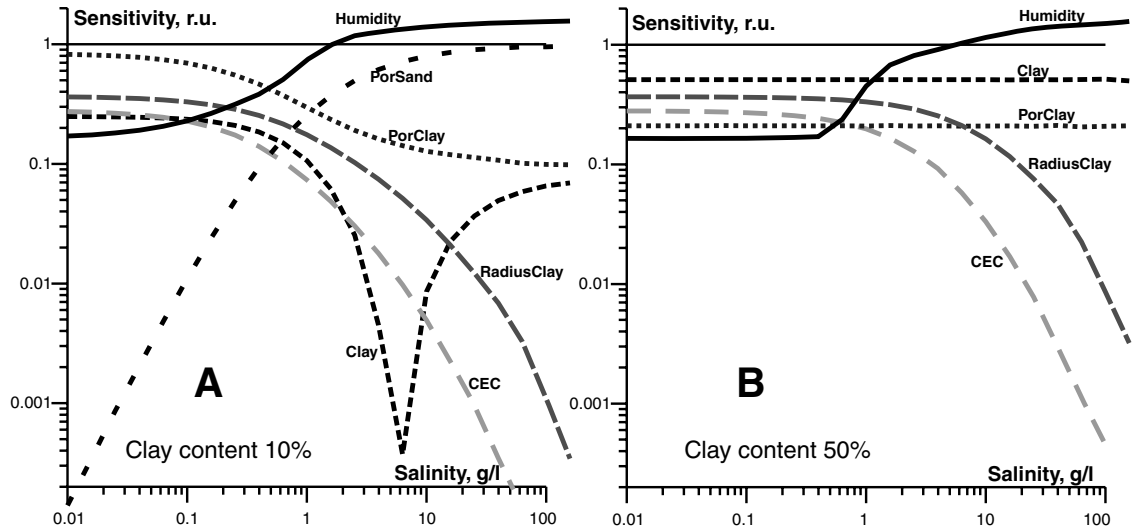

Figure 3 Sensitivity graphs for different model-parameters for two cases: clay content 10% and 50%. Parameters are: sand porosity = 25%, clay porosity = 55%, radius of sand capillaries = 10^{-4} m, radius of clay capillaries = 10^{-8} m, CEC of clay = 3 g/l, CEC of sand = 0.

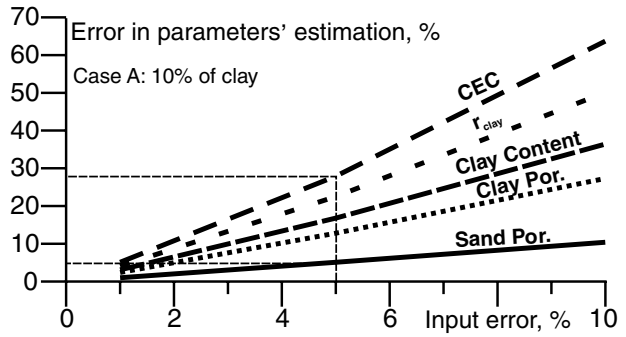

Figure 4 Errors in parameters estimation as a function of fitting error.

measured resistivity values to a fixed temperature T_0 of 20 °C, using the correction formula,

$$\rho_{20} = \rho(T)[1 + \alpha(T - T_0)], \tag{18}$$

where α is a temperature coefficient equal to 0.0177 1/ °C (Beklemishev 1963).

To estimate the equivalence of the model parameters, we calculated the correlation matrix in which the elements Φ_{ij}^{-1} demonstrate correlation between different model parameters.

Correlation values of less than 0.8 can be considered as weak and do not significantly affect the results. Only two correlation coefficients are above this limit for the 50% clay model. The maximum correlation coefficient of 0.92 corresponds to the clay porosity and clay content. The next highest of 0.91 corresponds to clay radii and CEC. For the 10% clay model, all correlation coefficients are below 0.8.

By using the principal diagonal terms of the covariance matrix Φ_{ii}^{-1}, we found the errors in the estimation of the parameters that are obtained by inversion, in the form of confidence intervals using the standard deviation of an error.

For input errors between 1% and 10% (the fitting error in interpretation), the errors in the parameter estimations are shown in Fig. 4. The sand and clay porosities and the clay content have much smaller errors than those for CEC and the clay capillary radius r_{clay}. The CEC has a maximal estimation error of <30% for a 5% input error.

VERIFICATION OF CLAY-CONTENT ESTIMATION USING CALIBRATED SAMPLES

The resistivities measured on calibrated sand-clay mixtures were used to verify the theoretical model, the accuracy of laboratory measurements, and the stability of inversion. We performed measurements with pure fine-grained silica sand, bentonite clay and mixtures of the two materials. The results are shown in Fig. 5.

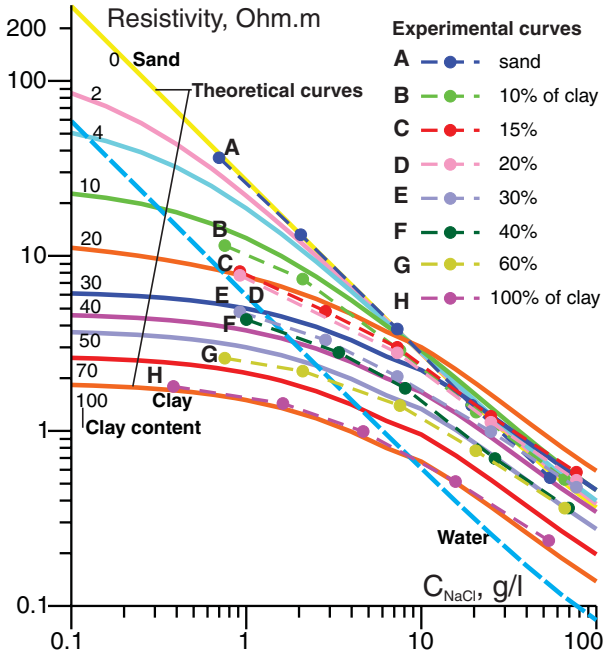

Figure 5 Resistivity measurements for pure sand, clay and their mixtures. Model parameters: CEC = 1.73 g/l, clay porosity = 55%, sand porosity = 22%, $r_{clay} = 3 \times 10^{-9}$ m.

Interpretation of these soil resistivity curves was performed by trying to minimize differences in sand and clay parameters for different mixtures (the fitting error between experimental and theoretical curves). The results of the interpretation are presented in Table 1.

The clay content was overestimated in the 10% to 40% range and was underestimated in the 60% to 100% range. In spite of some errors, the type of soil, whether sand, sandy loam, loam or clay, was in most cases found correctly. The mean error in the clay-content estimation was 19%.

SOME PRACTICAL EXAMPLES OF SOIL-RESISTIVITY MEASUREMENTS

We performed several soil-resistivity measurements on samples from different areas in Mexico using soil resistivimeters. For each sample, we prepared NaCl solutions with concentrations between 0.1 and 100 g/L. Each soil sample was separated into 4–5 equal parts in order to measure the soil resistivity at different water salinities. In this way, we obtained the resistivity versus salinity curve that could be fitted to the theoretical curves as shown in Figs 6 and 7.

Table 1 Results of $\rho(C)$ curve interpretation for calibrated samples

Sample	CEC of clay [%]	Clay content [%]	Soil porosity [%]	Clay radius [10^{-8} m]	Clay porosity [%]	Sand porosity [%]	Fitting error [%]
Sand		0	22	—	—	22	3.6
10% clay	1.4	14	21	0.3	55	27	3.5
15% clay	2.2	19	17	0.3	55	25	4.6
20% clay	1.4	22	18	0.3	55	28	3.6
30% clay	1.3	37	20	0.3	55	28	3.5
40% clay	1.5	49	28	0.3	55	28	4.9
60% clay	1.3	59	31	0.3	55	28	2.5
100% clay	1.8	98	50	0.3	53		3.1

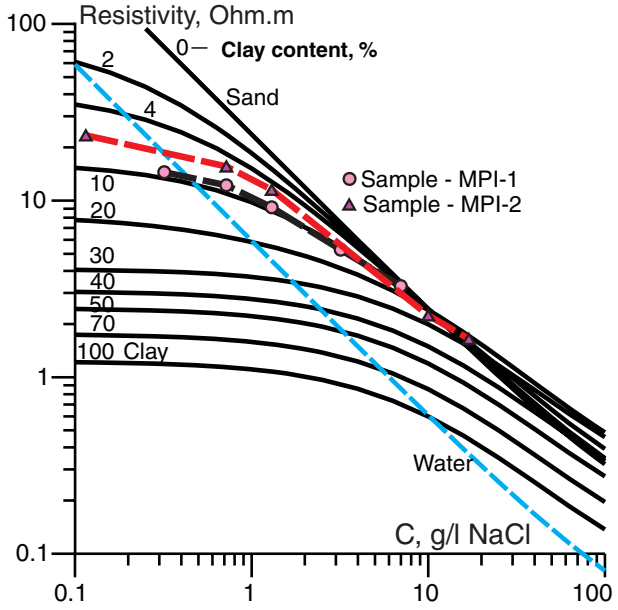

Figure 6 Experimental results and theoretical dependence of soil resistivity versus salinity. Theoretical model: clay porosity = 55%, sand porosity = 25%, $r_{sand} = 10^{-4}$ m, $r_{clay} = 10^{-8}$ m, $M = 0.75$. Experimental data: sample MPI-1: clay content = 9%, soil porosity = 30%, CEC = 7.2 g/l, fitting error = 3.2%; sample MPI-2: clay content = 6%, soil porosity = 31%, CEC = 7.2 g/l, fitting error = 5.5%.

Soil resistivities as a function of water salinity were interpreted quantitatively to find clay content, soil porosity, cation exchange capacity (CEC), sand and clay porosities, and sometimes capillary radii for the clay component. The results are presented in Table 2 and in Figs 6–8. Theoretical dependence is a function of many factors, such as clay content, the cation exchange capacity of clay, and the distribution of clay in the pores of sand. The final fitting error between experimental and theoretical curves was between 2% and 6%, depending on soil homogeneity.

Figure 6 shows the theoretical graphs and the measured resistivities as a function of water salinity for two samples of light sandy loam soil taken in the Mexican Petroleum Institute (MPI). The experimental resistivity measurements are marked with dashed lines and the experimental results with circles or triangles.

Figure 7 shows the results of clean soil samples from oil-contaminated sites: Campo-10 at Poza Rica, Veracruz (Shevnin *et al*. 2003) and Paredon-31 at Tabasco. Water samples gave water salinity of 1.2 g/L for case A and 0.22 g/L for case B (Fig. 7), while soil probes gave maximum clay contents of 63% for case A and 43% for case B. The combination of groundwater salinity and clay content (line D) gave us the resistivity interval E from 14 to 70 Ωm for uncontaminated soils. Next, we compared these data with statistical vertical electrical sounding results for both uncontaminated and contaminated zones (E and F), where the interval F is from 3 to 14 Ωm. The horizontal line separating these two zones is a boundary resistivity value for contamination mapping. For Campo–10, this boundary is 2.5 Ωm, and for Paredon-31 it is 14 Ωm (Fig. 7).

Measurements on three samples from uncontaminated (A) and contaminated (B, C) zones of Paredon-31 are shown in Fig. 8. The main difference between their petrophysical characteristics is in CEC values (0.12 g/L for sample A, 21 g/L for sample B and 8 g/L for sample C). We found that the CEC for clean soil is close to the real CEC value, whereas for contaminated soil, CEC values are much higher, and might be used as an oil-contamination indicator. The real cause might be the biodegradation of oil products (Abdel Aal *et al*. 2004), which resulted in an increase in superficial conductivity in the capillaries of the contaminated soil.

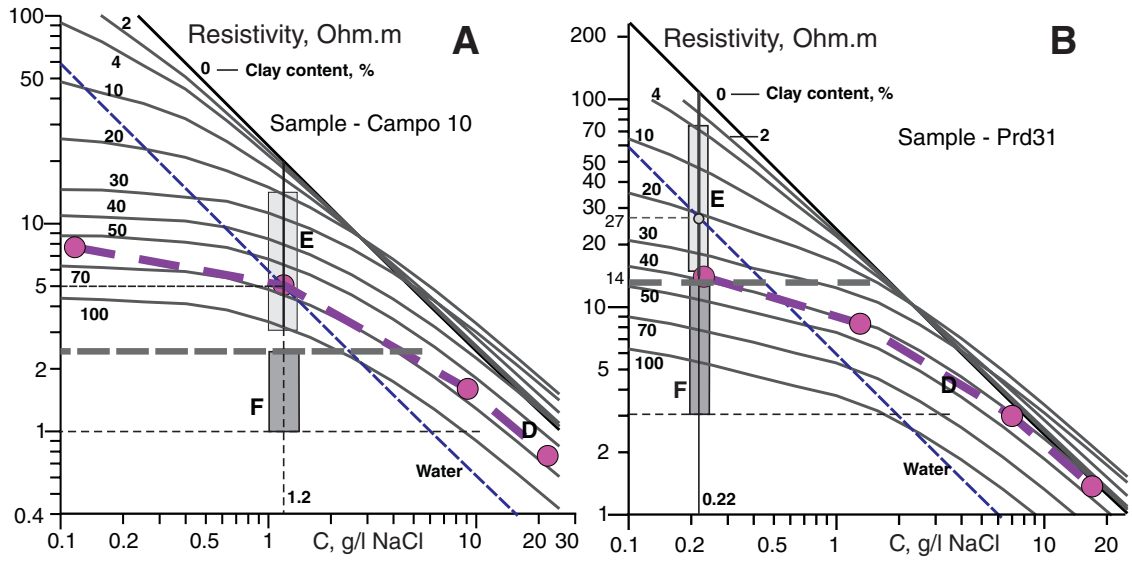

Figure 7 Petrophysical analysis for the sites Campo-10 (A) and Paredon-31 (B). Clay porosity = 55%, sand porosity = 25%, $r_{sand} = 10^{-4}$ m, $r_{clay} = 10^{-8}$ m, $M = 0.75$. Sample Campo-10: clay content = 63%, soil porosity = 44%, CEC = 0.45 g/l, fitting error = 2.9%. Sample Paradon-31: clay content = 43%, soil porosity = 33%, CEC = 0.12 g/l, fitting error = 2.1%.

Table 2 Results of parameter estimation for soil samples

N	Sample	Clay content [%]	Soil porosity [%]	CEC of clay [g/l]	Fitting error [%]
1	MPI-1	9	30	7.2	3.2
2	MPI-2	6	31	7.2	5.5
3	Campo-10	63	44	0.5	2.9
4	Paredon-31 (A)	43	33	0.1	2.1
5	Paredon-31 (B)	41	31	21	4.6
6	Paredon-31 (C)	41	31	8	2.8

Further development of petrophysical estimations of soil and water resistivity allowed us to recalculate resistivity cross-sections and to map them to those of petrophysical parameters, using interpreted resistivity and groundwater salinity. The results will be reported in a follow-up paper.

CONCLUSIONS

We have proposed a technique for clay-content estimation of weakly consolidated soils. This technique is based on the resistivity measurements of a sand-clay mixture at different water salinities, and on the inversion of resistivity data using the theoretical model developed in this study. To obtain soil parameters such as clay content, porosity and cation exchange capacity, it is necessary to perform up to five resistivity measurements for different water salinities in the range 0.6–100 g/L. The technique was validated by measurements on calibrated sand-clay mixtures and demonstrated an average error of 20% in clay-content estimation.

The practical application of this technique shows that determining the petrophysical parameters of the soil allows us to determine a boundary resistivity that separates clean and contaminated soils. This petrophysical information facilitates a better delimitation and characterization of oil-contaminated zones.

ACKNOWLEDGEMENTS

This work was possible due to the project 'Application of Electromagnetic Field Technology for Characterization of Oil-Contaminated Geological Media', within the framework of the Environmental and Industrial Safety Research Program of the Mexican Petroleum Institute.

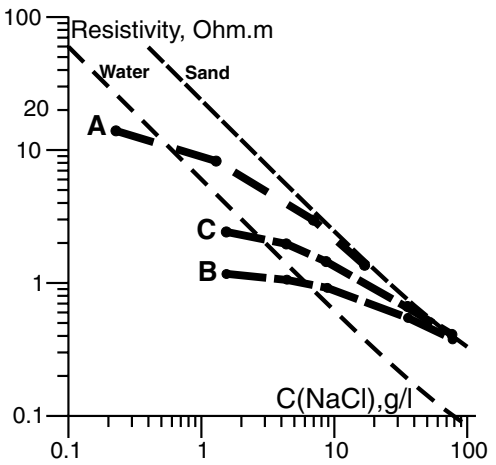

Figure 8 Three soil samples from Paredon-31 for a clean zone (A), a highly contaminated zone (B) and a moderately contaminated zone (C). Sand porosity = 25%, $r_{sand} = 10^{-4}$ m.

REFERENCES

Abdel Aal G.Z., Atekwana E.A., Slater L.D. and Atekwana E.A. 2004. Effects of microbial processes on electrolytic and interfacial electrical properties of unconsolidated sediments. *Geophysical Research Letters* **31** (12) (L12505), 10.1029/2004GL020030.

Beklemishev A.V. 1963. *Measures and Units of Physical Values*. Fizmatgiz, Moscow (in Russian).

Bussian A.E. 1983. Electrical conductance in a porous medium. *Geophysics* **48**, 1258–1268.

Clavier C., Coates G. and Dumanoir J. 1984. Theoretical and experimental bases for the dual-water model for interpretation of shaly sands. *SPE Journal*, April, 153–168.

Fridrikhsberg D.A. 1984. *A Course of Colloid Chemistry*. Khimija, Moscow (in Russian).

Goltsman F.M. 1971. *Statistical Models of Interpretation*. Moscow (in Russian).

Johnson D.L. and Sen P.N. 1988. Dependence of the conductivity of a porous medium on electrolyte conductivity. *Physical Review B* **37**, 3502–3510.

Klein K. and Santamarina J.C. 1997. Methods for broad-band dielectric permittivity measurements (soil-water mixtures, 5 Hz to 1.3 GHz). *ASTM Geotechnical Testing Journal* **20**, 168–178.

Klein K.A. and Santamarina J.C. 2003. Electrical conductivity in soils: Underlying phenomena. *Journal of Environmental and Engineering Geophysics* **8**, 263–273.

Knight R.J. 1991. Hysteresis in the electrical resistivity of partially saturated sandstones. *Geophysics* **56**, 2139–2147.

Kroit G.R. 1955. *Science of Colloids*. Innostrannaya Literatura, Moscow (in Russian).

de Lima O.A.L. and Sharma M.M. 1990. A grain conductivity approach to shaly sandstones. *Geophysics* **55**, 1347–1356.

Marion D. and Nur A. 1991. Pore-filling material and its effect on velocity in rocks. *Geophysics* **56**, 225–230.

Marion D., Nur A., Yin H. and Han D. 1992. Compressional velocity and porosity in sand-clay mixtures. *Geophysics* **57**, 554–563.

McGeary R.K. 1961. Mechanical packing of spherical particles. *Journal of the American Ceramic Society* **44**, 513–522.

Revil A., Cathles L.M., Losh S. and Nunn J.A. 1998. Electrical conductivity in shaly sands with geophysical applications. *Journal of Geophysical Research* **103** (B10), 23925–23936.

Revil A. and Glover P.W.J. 1998. Nature of surface electrical conductivity in natural sands, sandstones, and clays. *Geophysical Research Letters* **25**, 691–694.

Revil A., Grauls D. and Brévart O. 2002. Mechanical compaction of sand/clay mixtures. *Journal of Geophysical Research* **107** (B11), 2293. doi: 10.1029/2001JB000318.

Rhoades J.D., Raats P.A.C. and Prather R.J. 1976. Effects of liquid-phase electrical conductivity, water content and surface conductivity on bulk soil electrical conductivity. *Soil Science Society America Journal* **40**, 651–655.

Ryjov A.A. 1987. The main IP characteristics of rocks. *Application of IP Method for Mineral Deposits Research*, *Pp. 5–23. Moscow* (*in Russian*).

Ryjov A.A. and Sudoplatov A.D. 1990. The calculation of specific electrical conductivity for sandy-clayed rocks and the usage of functional cross-plots for the solution of hydro-geological problems. Scientific and Technical Achievements and Advanced Experience in the Field of Geology and Mineral Deposits Research, pp. 27–41. Moscow (in Russian).

Samstag F.J. and Morgan F.D. 1991. Induced polarization of shaly sands: Salinity domain modeling by double embedding of the effective medium theory. *Geophysics* **56**, 1749–1756.

Sen P.N. and Goode P.A. 1988. Shaly sand conductivity at low and high salinities. SPWLA 29th Annual Logging Symposium, Paper F.

Sen P.N., Scala C. and Cohen M.N. 1981. A self-similar model for sedimentary rocks with application to the dielectric constant of fused glass beads. *Geophysics* **46**, 781–795.

Shevnin V., Delgado-Rodríguez O., Mousatov A., Nakamura-Labastida E. and Mejía-Aguilar A. 2003. Oil pollution detection with resistivity sounding. *Geofísica Internacional* **42**, 603–622.

Tabbagh A., Panissod C., Guérin R. and Cosenza P. 2002. Numerical modeling of the role of water and clay content in soil and rock bulk electrical conductivity. *Journal of Geophysical Research* **107** (B11), 2318.

Tarantola A. 1994. *Inverse Problem Theory. A Method for Data Fitting and Model Parameter Estimation*. Elsevier. Science Publishing Co.

Taylor S. and Barker R. 2002. Resistivity of partially saturated Triassic sandstone. *Geophysical Prospecting* **50**, 603–613.

Waxman M.H. and Smits L.J.M. 1968. Electrical conductivities in oil-bearing shaly sands. *Journal of the Society Petroleum Engineering* **8**, 107–122.

Wyllie M.R.J. and Southwick P.F. 1954. An experimental investigation of the SP and resistivity phenomena in dirty sands. *Journal of Petroleum Technology* **6**, 44–57.

APPENDIX

Pore water conductivity in capillaries

The conductivity of brine relates strongly to salt type, concentration and temperature. Experimental data demonstrate that conductivity depends upon salinity and has three characteristic intervals: (1) at low concentrations of brine, the conductivity is directly proportional to the salt concentration; (2) in the high salinity range above 120 g/L (for NaCl), the conductivity becomes almost constant; (3) the conductivity begins to decrease slightly with further increases in salinity. Such behaviour of conductivity under electrical equilibrium can be represented as a function of cation and anion concentrations, and takes into consideration the hydration effect (Ryjov 1987), as follows:

$$\sigma_{\mathrm{w}} = F\left\{z_c U_{\mathrm{c}} C_c \exp\left(\frac{C_{\mathrm{c}}}{1000zn}\right) + z_{\mathrm{a}} U_{\mathrm{a}} C_{\mathrm{a}} \exp\left(\frac{C_{\mathrm{a}}}{1000zn}\right)\right\}, \tag{A1}$$

where $z_{\tilde{\mathrm{n}}}$ and z are charges of ions or valency, F is the Faraday number (96485 Q/mol), C_{c} and C_{a} are the cation and anion concentrations in water solution, U_{c} and U_{a} are the cation and anion mobilities, n is the hydration number, σ_{w} is the water conductivity.

This approach correctly predicts the conductivity of solutions for different salt types, such as NaCl, KCl, $Ca(HCO3)_2$, $CaCl_2$, $MgCl_2$, $CaSO_4$, $NaHCO_3$, Na_2SO_4, etc., for a wide concentration range (depending on solubility limits).

To evaluate the conductivity in the fine capillaries of clay, we applied an equation analogous to equation (A1), in which the concentration of the anions and cations is a function of the capillary radius and the cation exchange capacity for clay. The radial distribution of the conductivity in the capillary depends on the variation of the cation and anion concentrations, $C_{\mathrm{a}}(r)$ and $C_{\mathrm{c}}(r)$, respectively, in the pore. This equation is

$$\sigma(r) = F\left\{z_{\mathrm{c}} U_{\mathrm{c}} C_{\mathrm{c}}(r) \exp\left(\frac{C_{\mathrm{c}}(r)}{1000zn}\right) + z_{\mathrm{a}} U_{\mathrm{a}} C_{\mathrm{a}}(r) \exp\left(\frac{C_{\mathrm{a}}(r)}{1000zn}\right)\right\}. \tag{A2}$$

Here $C_{\mathrm{c}}(r)$ and $C_{\mathrm{a}}(r)$ are concentrations of cations and anions (in mol/m^3) as functions of the distance r from the capillary wall. This concentration also depends on the cation exchange capacity (CEC) of the solid component. Specifically, $C_i(r) = C_i^{\mathrm{EDL}}(r) + C_i^{\mathrm{CEC}}(r)$, where the index i indicates specific cations or anions.

The electrical double layer (EDL) depends mainly on the ion concentrations and is calculated for each salt concentration. The cation exchange capacity depends primarily on the properties of the solid. In other words, we can change ion concentrations and the resulting electrical double layer with the type of solution, but we cannot change the cation exchange capacity.

The estimation of the concentration distribution $C_i(x)$ for one ion type with charge z_i (anions or cations) in a electrical double layer is based on the Boltzmann equation that follows the theory developed by Langmuir, Frumkin and Stern (Fridrikhsberg 1984), i.e.

$$C_i(x) = C_{0i} \exp(-z_i F \psi(x)/RT), \tag{A3}$$

where C_{0i} is the cation or anion concentration in an electroneutral solution, x is the shortest distance from a given point in a liquid phase to a solid surface, $\psi(x)$ is the electric potential in a fluid at a given distance x from the capillary wall, R is the gas constant, and T is the absolute temperature (K).

The electric potential ψ as function of distance x from the capillary wall is determined by the charge distribution in the electrical double layer and the cation exchange capacity of the solid phase. This function can be found from the Poisson–Boltzmann equation:

$$\nabla^2 \psi(\mathbf{x}) = \frac{\rho(\mathbf{x})}{\varepsilon \varepsilon_0}, \tag{A4}$$

where $\rho(\mathbf{x}) = \sum_i z_i F C_i(\mathbf{x})$ is the sum of ion charges at a distance x, ε is the relative dielectric constant of a fluid and ε_0 is the permeability of a vacuum (8.854×10^{-12} F/m).

For a flat electrical double layer, the Poisson-Boltzmann equation (A4) becomes simpler, as it depends on only one coordinate, $\times = \{x_1, 0, 0\}$. Under phase boundary conditions:

$$\text{when } x \to \infty, \quad \text{then } \psi_1 = 0$$
$$\text{and } \mathrm{d}\psi/dx = 0; \quad \text{when } x = x_0, \quad \text{then } \psi = \psi_1, \tag{A5}$$

where ψ_1 refers to the Stern potential. Its value is determined at a distance x_0 from the solid phase, i.e. the ion radius. The one-dimensional equation simplifies to

$$\frac{\mathrm{d}^2 \psi(x)}{\mathrm{d}x^2} = -\frac{F}{\varepsilon \varepsilon_0} \sum_i z_i C_{0i} \exp(-z_i F \psi(x)/RT), \tag{A6}$$

and has the exact solution (Kroit 1955),

$$\tanh\left(\frac{zF\psi(x)}{4RT}\right) = \exp\left(\frac{x}{\delta}\right) \tanh\left(\frac{zF\psi_1}{4RT}\right), \tag{A7}$$

where $\delta = \frac{\sqrt{\varepsilon RT/8\pi C}}{zF}$ is the Debye distance, which is a measure of the thickness of a diffusive layer.

At small values of the argument ($zF\psi/4RT$), decomposition of the expression (A7) into a series, results in the simple formula,

$$\psi = \psi_1 \exp\left(\frac{-x}{\delta}\right), \tag{A8}$$

from which it follows that at $x = \delta$, the value of the potential ψ is e ($= 2.7\ldots$) times smaller than the Stern potential, i.e. $\psi = \psi_1/e$.

The potential of a liquid, $\psi = \psi\ (x)$, at any point depends on the distance x, which is measured from a solid phase up to the given point. This potential can be calculated by the solution of the non-linear equation (A7). The solution can be found if the value ψ_1 and also the fluid parameter C (the ion concentration) and ε, R, T and F are known.

According to adsorption theory, the Stern potential depends on the number of ions directly adjacent to a solid phase, i.e. a specific adsorption factor Γ_0, which determines the density of specifically adsorbed ions on a unit surface. The relationship between the Stern potential and the degree of ionic adsorption on a surface is determined by the following system of non-linear equations:

$$\begin{aligned} &\sinh\left(\frac{zF\psi_1}{2RT}\right) = (\sqrt{\pi/2\varepsilon RTC})\sum_i z_i F\Gamma_i, \\ &\Gamma_i = \Gamma_{0i}\frac{N\exp\left(-\Phi_i + \dfrac{\pm z_i F\psi_1}{RT}\right)}{1 + N\exp\left(-\Phi_i + \dfrac{\pm z_i F\psi_1}{RT}\right)}, \end{aligned} \tag{A9}$$

where Γ_i is the degree of ion adsorption on the surface (in mol/m^3), Γ_{0i} is the limit of the number of adsorption places on a unit surface (in mol/m^3); $\Phi_i = zFU_i/RT$ is a dimensionless potential describing the specific adsorption potential, U_i is the electric potential of this adsorption, and N is the relative degree of adsorption. The value of the Stern potential can be found by solving the system (A9).